Modelling and Simulation of Vibrocompaction Processes

Javier González-Carbajal, Daniel García-Vallejo, Jaime Domínguez
Department of Mechanical Engineering and Manufacturing, Faculty of Engineering of Seville, Spain.

Summary. This paper focuses on the vibrocompaction process of quartz agglomerates, where unbalanced motors are used to compact a quartz-resin mixture. A nonlinear model is introduced which includes some of the main nonlinearities present in the real system: the nonideal interaction between the motors and the vibrating system , contact and impacts between mixture and piston (the platform upon which the motors are mounted) and also between the mixture and the supporting mould, and a nonlinear constitutive law for the mixture, which allows modelling the compaction itself. By numerically solving the system of differential equations corresponding to this model, some insight into the system nonlinear behaviour is obtained, with special interest in the influence of different factors on the final level of compaction achieved.

Introduction

Vibrating machines are extensively used as a means to compact granular materials, with applications in geotechnics, manufacturing and other engineering areas. In particular, this paper has been motivated by the interest of the authors in a particular manufacturing process, where a quartz-resin mixture is compacted by using the vibration produced by a set of unbalanced motors, together with a vacuum system.

Quartz agglomerates, made of granulated quartz mixed with a polyester resin, are widely used as an artificial stone for countertops in kitchens or bathrooms. The manufacturing process of a slab of this material starts with the filling of a mould with the mixture of quartz and resin. Once the mould is full, a conveyor belt carries it to the vibrocompaction zone, where the thickness of the slab is reduced to nearly half of its initial value, by eliminating the air out of the material. Then, the mixture is cured in a kiln, during a specified time interval, at a suitable temperature for the polymerization of the resin. After the resin is polymerized, an air stream is used to cool the slab before it enters the mechanical finishing stage. During this process the edges are cut, producing a slab of prescribed dimensions, and the surfaces are polished. Then, the product is ready for the quality control stage.

It is worth giving some more insight into the vibrocompaction stage of the process, which is the one of interest for the purpose of this study. Before the mixture has been compacted, it is composed of three different phases: solid (the quartz grains), liquid (the resin) and gas (air). The air is present in the material in two different ways: as bubbles within the resin or as gaps between grains of quartz that the resin has not been able to fill. The aim of the compaction process is to eliminate the air out of the mixture, since the presence of pores at the surface of the final countertop is clearly detrimental from a practical point of view: the pores tend to accumulate dirt and are rather difficult to clean.

The compaction is conducted by means of several unbalanced electric motors, mounted on a piston with the dimensions of the slab surface. At the beginning of the vibrocompaction process, the piston descends onto the mixture and exerts a static pressure, due to its weight and to an air pressure applied on it. Then, the air pressure inside the mould is reduced by using a vacuum system, after which the motors are switched on. The vibration produced by the unbalanced motors is the main responsible for the compaction. During the motion of the system, there can be separations and impacts between the piston and the slab, which are generally beneficial for the compaction, as they produce very high peaks of compression forces. In order to reduce vibrations in the vicinity of the compaction machine, elastic elements are placed between the foundation of the machine and the ground, acting as a vibration absorber and thus protecting nearby equipment. Fig. 1 shows a pilot plant used for testing purposes, which preserves the main features of the actual industrial machine. It is interesting to note that there are two motors mounted on the piston, which rotate in opposite directions in order to cancel the horizontal components of the centrifugal forces on the unbalanced masses. Hence the net effect of the rotation of both motors is an oscillating vertical force.

From the above comments, it is clear that the vibrocompaction process is extremely complex from a physical point of view. A large number of factors –some of them being intrinsically nonlinear– influence the final result of the compaction:

- The quartz granulometry, the rheological properties of the resin and the mass ratio between quartz and resin affect the mechanical behaviour of the compacting mixture. This behaviour is necessarily nonlinear, since the mixture suffers irreversible deformation during compaction. Moreover, an accurate description of this constitutive law would require modelling the motion of the bubbles through the mixture, the friction between quartz particles, the interaction between quartz and resin, etc. Some investigations about suitable constitutive laws for compacting materials can be found in [1–7].
- The dynamic properties of the different elements of the machine –the piston, the conveyor belt supporting the mould, the elastomer between the foundation and the ground, etc. – may influence the vibrocompaction as well.
- The speed of the motors, their available power and the amount of unbalance are key parameters of the process.
- The final result of the compaction may also depend on the duration of the process.
- The spatial distribution of the vacuum channels influences the extraction of the air out of the mixture, thereby affecting the compaction.

In addition to the mentioned sources of nonlinearity, it is known that, when a structure is excited by one or more unbalanced motors, some particular nonlinear effects can take place due to the interaction itself between the exciter and the vibrating system [8–11]. The main idea is that, in general, the motion of the unbalanced motor will be influenced by the response of the vibrating system, due to the inertia forces that the vibration produces on the unbalanced mass [11]. Then, rather than a known excitation acting on the vibrating system, what we generally have is a two-way coupling between the motions of the exciter and the structure. In most of the scientific literature, this is called a nonideal excitation [12–14], and the associated nonlinear phenomena are usually referred to as The Sommerfeld effect [15–17]. Conversely, an excitation is said to be ideal if it remains unaffected by the vibrating response.

After the works of Sommerfeld and Kononenko, many investigations have been conducted in order to better understand and predict the effect of nonideal excitations on vibrating systems.

Rand et al. [19] reported the detrimental effect of a nonideal energy source in dual spin spacecrafts, which could endanger a particular manoeuvre of the spacecraft, once placed in orbit. They also designed suitable nonlinear controllers to minimize this kind of undesired channelling of energy [20].

Although most studies use averaging procedures to obtain approximate solutions to the equations of motion, Blekhman [9] proposed an alternative approach, based on the method of 'Direct Separation of Motions'.

Several authors, like El-Badawi [16], Bolla et al. [14] and González-Carbajal et al. [11,18], analysed models where the vibrating system included an intrinsic cubic nonlinearity, in addition to the nonlinearity associated to the nonideal coupling between exciter and structure.

Balthazar et al. [12] published an extensive exposition of the state of the art concerning nonideal excitations.

Considering the vibrocompacting machine for quartz agglomerates, it is reasonable to expect that nonlinear effects, produced by a nonideal coupling between the vibrating system and the unbalanced motors, are present in the system behaviour. The model presented in this paper will allow showing how these phenomena, associated to nonideality of the energy source, can affect the result of the compaction process.

Description of the model

The aim of this Section is to present an approximate model which, without intending to give accurate quantitative predictions, provides useful qualitative results regarding the vibrocompaction process. This may be seen as a first step towards the ambitious goal of achieving a more complex model which reliably captures the dynamics of the real system.

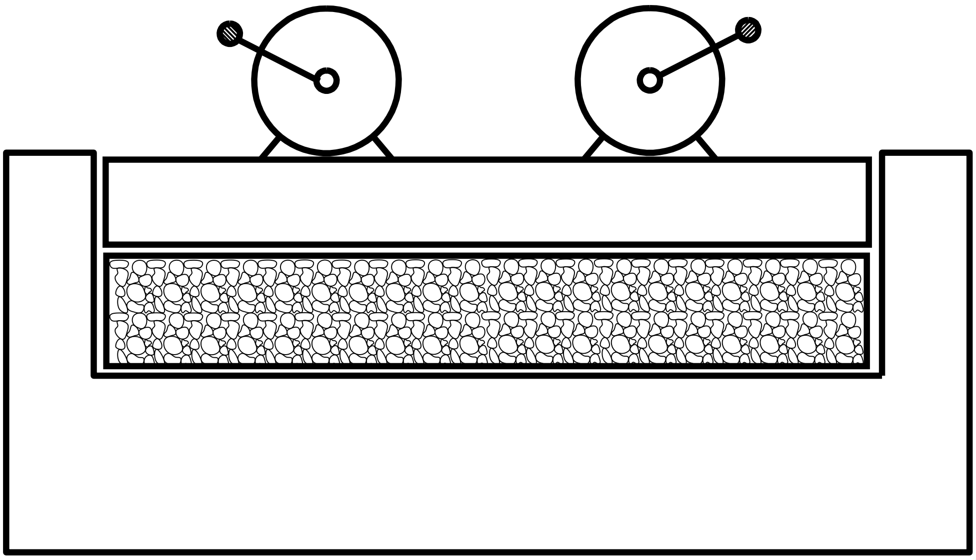

Fig. 1 Simplified representation of the compacting machine

The simplification carried out can be observed in

Fig. 1 and Fig. . The former shows a schematic picture of the real machine, while the later displays the approximate 4-DOF model. The quartz-resin mixture is represented in the model by a couple of masses attached to each other by a linear damper and a nonlinear spring, which models the compaction itself by allowing for permanent deformation when the spring is compressed. Then, the distance between both masses would represent the thickness of the compacting mixture. The mould is modelled as a rigid base, while the piston with the unbalanced motors is represented by a mass with a single unbalanced motor. The mixture is in contact –with separations and impacts allowed– with the mould at the bottom and with the piston at the top. The vacuum system is not included in the model.

It should be noted that the model assumes the horizontal motion of the piston to be completely restrained, which makes unnecessary to include a couple of motors rotating in opposite directions.
As represented in Fig. , the model has 4 DOFs: y_b, y_t, y_p and ϕ, which correspond, respectively, to position of the bottom of the mixture, position of the top of the mixture, position of the piston and rotation of the motor.
The parameters represented in Fig. are as follows: m_m stands for the mass of the mixture, m_1 is the unbalanced mass, m_p is the mass of the piston and the motor, r is the eccentricity of the unbalance, I_o is the rotor inertia, b is the damping coefficient, F_m is the force produced by the nonlinear spring and g is the gravity constant.

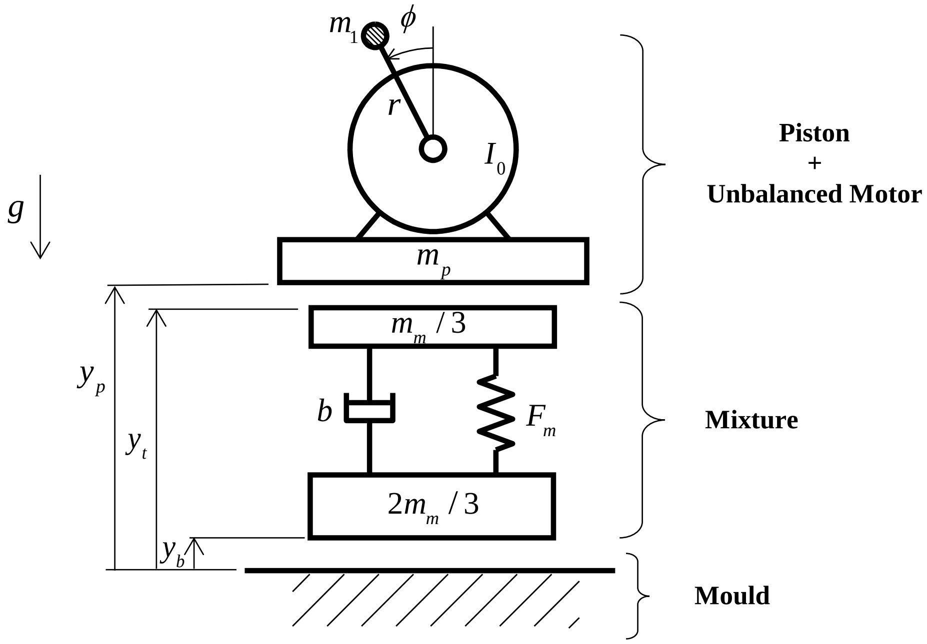

Fig. 2 – 4-DOF model of the vibrocompaction process

Notice that the total mass of the mixture is distributed in the proposed model in a particular way: one third corresponds to the upper mass and two thirds to the bottom mass. In order to understand this feature of the model, suppose that, in the real system, the bottom of the mixture is in continuous contact with the mould and, therefore, remains at rest during the system vibration. Assume also that the mass of the mixture is uniformly distributed over the slab thickness. Then, if the deformation is uniform over the slab thickness as well, the effective mass of the mixture during the oscillations can be shown to be one third of its total mass. Note that the assumption of uniform deformation is suitable because the mass of the piston is much greater than that of the mixture and, consequently, it is reasonable to approximate the deformed shape by that corresponding to a concentrated load on the top surface of the slab.
Obviously, if the top mass contains one third of the total mass of the mixture, there have to be two thirds at the bottom mass: when there are separations between mixture and mould and between mixture and piston, it must be the total mass of the slab which moves freely.
The driving torque provided by the motor minus the losses torque due to friction at the bearings and windage is assumed to be a linear function of the rotor speed:

$$L_m(\dot{\phi}) = A + D\dot{\phi}, \tag{1}$$

with $A > 0$, $D < 0$.

The equations of motion of the system can be obtained by either equilibrium considerations or any other analytical mechanics approach like Lagrange's method or Hamilton's principle:

$$\left\{\begin{array}{c} (m_p + m_1)\ddot{y}_p = m_1 r(\dot{\phi}^2\cos\phi + \ddot{\phi}\sin\phi) + F_{ct} - (m_p + m_1)g \\ \dfrac{m_m}{3}\ddot{y}_t + F_m + b(\dot{y}_t - \dot{y}_b) = -F_{ct} - \dfrac{m_m}{3}g \\ \dfrac{2m_m}{3}\ddot{y}_b - F_m - b(\dot{y}_t - \dot{y}_b) = F_{cb} - \dfrac{2m_m}{3}g \\ I\ddot{\phi} = L_m(\dot{\phi}) + m_1 r\sin\phi\,(\ddot{y}_p + g) \end{array}\right\}, \tag{2}$$

where $I \equiv I_0 + m_1 r^2$ and F_{cb}, F_{ct} represent the normal contact force between mixture and mould and between mixture and piston, respectively. Clearly, the most challenging features of this model are the behaviour of the nonlinear spring and the computation of the contact forces. System (2), together with the definition of the spring force and the contact forces given in the following, constitutes the proposed model for the compacting machine.
A Hunt and Crossley nonlinear contact model of the form

$$F_c = k_c \delta^n + b_c \delta^p \dot{\delta}^q, \tag{3}$$

Is used, where it is standard to set $n = p$, $q = 1$. Note that the damping term depends on indentation, which is physically sound, since plastic regions are more likely to develop for larger contact deformations. Moreover, the contact force does not exhibit discontinuous changes at the impact and separation instants, thereby overcoming one of the main problems of the spring-dashpot model.

Numerical results

In this section, system (2) is numerically solved for different scenarios. The chosen initial conditions for all the simulations correspond to the static equilibrium position of the system:

$$\left\{\begin{matrix} \phi(0) = \pi \\ \dot{\phi}(0) = 0 \\ y_b(0) = d_b \\ \dot{y}_b(0) = 0 \\ y_t(0) = d_b + L_0 + d_{st} \\ \dot{y}_t(0) = 0 \\ y_p(0) = d_b + L_0 + d_{st} + d_t \\ \dot{y}_p(0) = 0 \end{matrix}\right\}, \tag{4}$$

where d_t and d_b are the indentations at the top and bottom contacts, respectively, due to the weight of the elements above the contact.
With this initial configuration, system (2) is solved, using embedded Runge-Kutta formulae of orders 4 and 5, for a simulation time t_f which varies between $30s$ and $55s$. This total time includes three different stages in the simulation, of respective lengths t_1, t_2 and t_3 $\left(t_f = t_1 + t_2 + t_3\right)$:
- During the first stage $(0 \le t < t_1)$ parameter A is linearly increased from A_0 to A_f, with A_0 and A_f being defined for each particular simulation. The slope D is kept constant along the process, which implies that the motor characteristics is displaced parallel to itself. Then, at this stage, the motor is being controlled as in Sommerfeld's experiment.
- At the second stage $(t_1 \le t < t_1 + t_2)$, parameter A is kept constant at its final value A_f. During this stage, the machine is expected to reach a stationary operating point.
- At time $t = t_1 + t_2$, the motor is switched off in order to let the system reach a compacted equilibrium position.

Clearly, once the motor is switched off, there is no driving torque on the rotor, and function $L_m\left(\dot{\phi}\right)$ must only account for the resisting torque due to windage and friction at the bearings. This is modelled by replacing the motor characteristic with the following curve:

$$L_m\left(\dot{\phi}\right) = 0.2 \cdot D\dot{\phi}, \qquad \text{for } t_1 + t_2 \le t < t_f. \tag{5}$$

Hence it is being assumed that the slope of the resisting torque curve is 20% of the slope of the motor characteristic.
Parameters t_2 and t_3 have been chosen as $15s$ for all the simulations, while t_1 will take different values depending on the case under study.

The proposed model (2) is defined by 11 dimensional parameters

$$\left\{m_1, m_p, m_m, b, r, I_0, d_f, F_f, R_k, k_c, b_c\right\}, \tag{6}$$

besides the two parameters associated to the motor control

$$\{A, D\}. \tag{7}$$

For this first simulation, the set of parameters (6) is chosen as

$$\begin{Bmatrix} m_1 = 20\text{kg}, & m_m = 240\text{kg}, & m_p = 1.5 \cdot 10^3\text{kg} \\ r = 0.1\text{m}, & I_0 = 0.84\text{kgm}^2, & b = 4 \cdot 10^3\ \text{Ns/m} \\ d_f = -0.1\text{m}, & F_f = -1 \cdot 10^5\text{N}, & R_k = 0.1 \\ k_c = 3 \cdot 10^9\ \text{N/m}\,, & b_c = 9.5 \cdot 10^6\ \text{Ns/m} & \end{Bmatrix}. \quad (8)$$

Before the numerical resolution of the equations of motion, it is useful to obtain some previous information about the system. First, from the knowledge of parameters $\{d_f, F_f,\ R_k\}$, stiffnesses k_0 and k_f can be computed as:

$$k_0 = 1.82 \cdot 10^5\ \text{N/m}\,, \qquad k_f = 1.82 \cdot 10^6\ \text{N/m} \quad (9)$$

The, the initial stiffness for the dynamic process can also be obtained, together with the static compaction:

$$k_{st} = 7.39 \cdot 10^5\ \text{N/m} \Rightarrow \gamma_{st} = 34.1\%. \quad (10)$$

A numerical experiment is carried out now, where the motor control parameters are chosen as $t_1 = 10\text{s},\ D = -5\text{Nms},\ \text{A}_0 = 20\text{Nm},\ \text{A}_f = 140\text{Nm}$.
The results of the simulation are represented in Fig. 3 and Fig. .

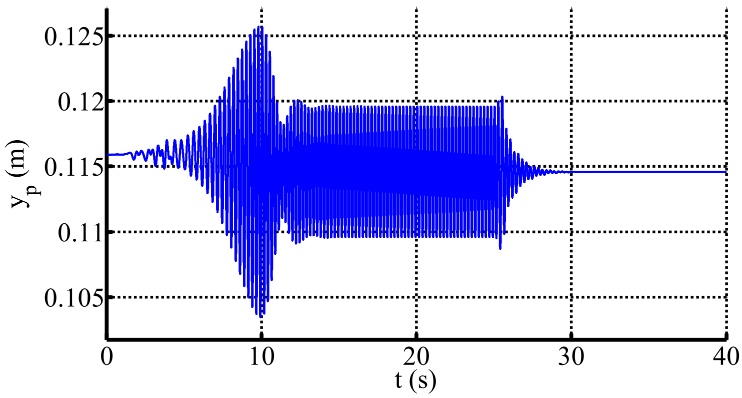

Fig. 3 Piston displacement

It is observed in Fig. 3 that, as the motor curve is displaced upwards between 0 and 10s, the oscillation amplitude grows monotonically, until a point where a jump phenomenon is encountered. After the jump, the system clearly reaches a post resonant state of motion, as shown in Fig. , where ω_{np} represents the natural frequency of the system during the stationary motion of stage 2.
The jump phenomenon encountered here clearly resembles the Sommerfeld effect explained in the introduction. However, it might be somehow different to the general phenomenon since no clear slowing down in the increase of the rotor speed is observed in Fig. . This is probably due to the additional complexity of the vibrocompaction.

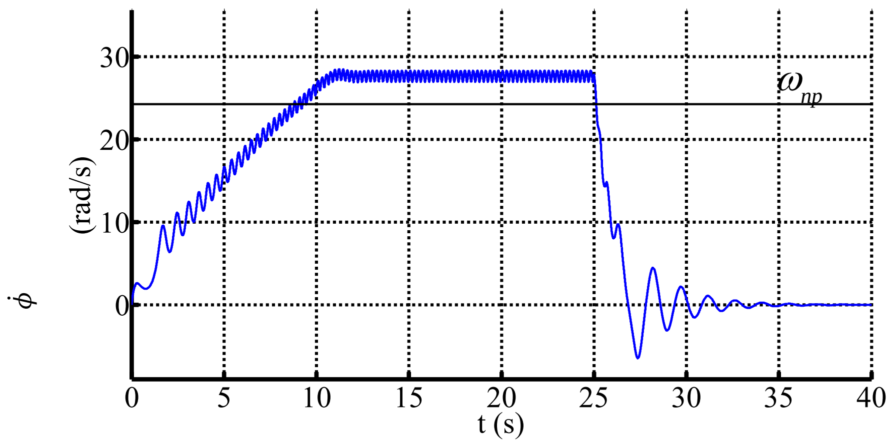

Fig. 4 Rotor speed

Note the difference between the initial and final position of the piston in Fig. 3, which reveals the compaction due to vibration. Regarding the top and bottom contacts, no separations or impacts were found in this case. Hence the displacements of the mixture, which do not give much significant information, have not been represented.

Conclusions

A novel nonlinear model for the vibrocompaction of quartz agglomeartes is proposed in this work. As far as the authors know, this is the first attempt to model this industrial process by using nonlinear systems analysis techniques, including both perturbation and averaging technics. In addition, by numerically solving the equations of motion for several sets of parameters, the effect of different parameters of the process in the final level of compaction achieved is investigated.

References

[1] S. Pietruszczak, G.N. Pande, Constitutive Relations for Partially Saturated Soils Containing Gas Inclusions, J. Geotech. Eng. 122 (1996) 50–59. doi:10.1061/(ASCE)0733-9410(1996)122:1(50).

[2] E.E. Alonso, A. Gens, A. Josa, A constitutive model for partially saturated soils, Géotechnique. 40 (1990) 405–430. doi:10.1680/geot.1990.40.3.405.

[3] J.J. Stickel, R.L. Powell, Fluid Mechanics and Rheology of Dense Suspensions, Annu. Rev. Fluid Mech. 37 (2005) 129–149. doi:10.1146/annurev.fluid.36.050802.122132.

[4] P. Richard, M. Nicodemi, R. Delannay, P. Ribiere, D. Bideau, Slow relaxation and compaction of granular systems, Nat Mater. 4 (2005) 121–128. http://dx.doi.org/10.1038/nmat1300.

[5] N. Favrie, S. Gavrilyuk, Dynamic compaction of granular materials, Proc. R. Soc. A Math. Phys. Eng. Sci. 469 (2013). http://rspa.royalsocietypublishing.org/content/469/2160/20130214.abstract.

[6] Kiesgen de Richter, S., Hanotin, C., Marchal, P., Leclerc, S., Demeurie, F., Louvet, N., Vibration-induced compaction of granular suspensions, Eur. Phys. J. E. 38 (2015) 74. doi:10.1140/epje/i2015-15074-7.

[7] J.B. Knight, C.G. Fandrich, C.N. Lau, H.M. Jaeger, S.R. Nagel, Density relaxation in a vibrated granular material, Phys. Rev. E. 51 (1995) 3957–3963. doi:10.1103/PhysRevE.51.3957.

[8] V.O. Kononenko, Vibrating Systems with a limited power supply, Illife, London, 1969.

[9] I.I. Blekhman, Vibrational Mechanics-Nonlinear Dynamic Effects, General Approach, Singapore, 2000.

[10] M.F. Dimentberg, L. Mcgovern, R.L. Norton, J. Chapdelaine, R. Harrison, Dynamics of an Unbalanced Shaft Interacting with a Limited Power Supply, Nonlinear Dynamics. (1997) 171–187. doi:10.1023/a:1008205012232.

[11] J. González-Carbajal, J. Domínguez, Limit cycles in nonlinear vibrating systems excited by a nonideal energy source with a large slope characteristic, Nonlinear Dynamics. (2016). doi:10.1007/s11071-016-3120-7.

[12] J.M. Balthazar, D.T. Mook, H.I. Weber, B. R., A. Fenili, D. Belato, J.L.P. Felix, An Overview on Non-Ideal Vibrations, Meccanica. 38 (2003) 613–621.

[13] J.L.P. Felix, J.M. Balthazar, M.J.H. Dantas, On energy pumping, synchronization and beat phenomenon in a nonideal structure coupled to an essentially nonlinear oscillator, Nonlinear Dynamics. 56 (2009) 1–11. doi:10.1007/s11071-008-9374-y.

[14] D.T. Bolla, M. R., Balthazar, J. M., Felix, J. L. P., Mook, On an approximate analytical solution to a nonlinear vibrating problem , excited by a nonideal motor, Nonlinear Dynamics. (2007) 841–847. doi:10.1007/s11071-007-9232-3.

[15] L. Munteanu, C. Brişan, V. Chiroiu, D. Dumitriu, R. Ioan, Chaos–hyperchaos transition in a class of models governed by Sommerfeld effect, Nonlinear Dynamics. 78 (2014) 1877–1889. doi:10.1007/s11071-014-1575-y.

[16] A.A. El-Badawy, Behavioral Investigation of a Nonlinear Nonideal Vibrating System, Journal of Vibration and Control. 13 (2007) 203–217. doi:10.1177/1077546307073674.

[17] J.L.P. Felix, J.M. Balthazar, Comments on a nonlinear and nonideal electromechanical damping vibration absorber, Sommerfeld effect and energy transfer, Nonlinear Dynamics. 55 (2009) 1–11. doi:10.1007/s11071-008-9340-8.

[18] J. González-Carbajal, J. Domínguez, Nonlinear Vibrating Systems Excited by a Nonideal Energy Source with a Large Slope Characteristic, Mech. Syst. Signal Process. (2017).

[19] R.H. Rand, R.J. Kinsey., D.L. Mingori, Dynamics of spinup through resonance, International Journal of Non-Linear Mechanics. 27 (1992) 489–502. doi:10.1016/0020-7462(92)90015-Y.

[20] R.J. Kinsey, D.L. Mingori, R.H. Rand, Nonlinear Controller to Reduce Resonance Effects during Despin of a Dual-Spin Spacecraft through Precession Phase Lock, Proc. 31st Conf. Decis. Control. (1992).